MATHEMATICAL ANALYSIS OF DYNAMICAL MODEL OF MICROALGAL GROWTH FOR BIOFUEL PRODUCTION

[1]R. Karthikeyan,[2]A.P.Dhanabalan,[3]M. Rasi,[4]L.Rajendran
[1,2] PG and Research Department of Mathematics, AlagappaGovt Arts College, Karaikudi-630003, Tamilnadu, India.
[3]Department of Mathematics, Lady Doak College, Madurai-625007, Tamilnadu, India
[4]Department of Mathematics ,Academy of Maritime Education and Training (AMET),
Deemed to be University, Kanathur- 603112, Tamilnadu, India

Abstract :Modelling of microalgal growth for biofuel production is discussed. The model proposed herein is a dynamical model of microalgal lipid production under nutrient limitation. In this paper, approximate analytical expressions for the concentration of nitrate (substrate), biomass and quotas of lipid, sugar, functional are obtained for all values of the parameters using a new Homotopy perturbation method (HPM). Numerical solutions have also been presented in order to explain the behavior of the system. A comparative study of the approximate analytical solution with numerical solution and experimental data confirm that the proposed model is consistent in the region of approximation.

Keywords - Biofuel; mathematical modelling; non-linear equations; microalgal production; HPM.

I. INTRODUCTION

There has been a considerable interest amongst the researecher towards the production of biofuel due to its role in mitigating industrial CO_2 emitted from power plants, cement plants, etc. As a consequnce of decrease in the production of oil and natural gas, there is a growing demand for the production of energy sources such as biofuels [1]. The chief sources of biofuels include cellulose, microalgae, soy, corn, sugarcane, animal fat, paper waste etc. Of these, microalgae is considered as the best source due to its wide spread availability, high growth in short span of time and high biomass production within minimum land [2]. In addition, it can store up to 50% of their body weight in fat which can be converted into oil for ethanol production.

Microalgae are microscopic and they are usually found in freshwater and marine systems. They are unicellular species which exist either individually, or in chains/groups. It has been considered as the third generation feedstock for biofuel production [3]. The use of microalgae as an alternative biofuel feedstock has gained interest from researchers, entrepreneurs and the public [4]. Microalgae-based biofuels have several sustainability, economic, and environmental benefits over other available conventional biofuels [5]. Microalgae are considered as the largest biomass producers due to higher neutral lipid content thereby it negates the choice of other terrestrial plants for biofuel production [7].

Bernard et al. [3] discussed the challenges and hurdles to improve microalgae based biofuel production. Quinn et al. [4] reported a literature-based bulk growth model incorporating the primary factors that affect microalgae growth and lipid accumulation. Ho et al. [5] reported the feasibility of using carbohydrate-producing microalgae as feedstock for fermentative bioethanol production. Sukenik et al. [9, 10] proposed the first dynamical model for microalgal production pond and later included the time-discrete photo acclimation dynamics. In a review, Bernard et al. [3] summarized all the possible microalgae dynamical models including the Droop model [11]. Recently, Mairet et al. [12] proposed a dynamical model of microalgal lipid production under nitrogen limitation. However, to the best of our knowledge, no rigorous analytical solutions to any of these models have been reported. The purpose of this communication is to provide an approximate analytical expression for the concentration of nitrate (substrate), biomass and quotas of lipid, sugar, functional for various values of the parameters. The results will then be used to optimize other models of microalgae growth in the perspective of large scale biofuel production.

II. MATHEMATICAL FORMULATION

Figure 1ª. represents the schematic diagram for the carbon flow. The simplified scheme for low and constant free fatty acid (FFA) quota is represented in Figure 1b. Here, the growth of microalgae whose biomass in terms of organic carbon is denoted by x. These microalge are limited by an inorganic nitrogen s.Nutrient uptake is done by microalgae at the rate $\rho(s)$. The mathematical expression for the specific growth rate is denoted as $\mu(q_n)$. In 1990, Bastin and Dochain [13] summarized the main mass transfer of carbon and nitrogen by means of the differential equations. Based on this model, Mairet et al[12] developed the rate equation for the concentration of nitrate s, nitrogen quota q_n, carbon biomass x, quotas of neutral lipid q_l and functional quota q_f as follows:

$$\frac{ds}{dt} = D\,s_{in} - \rho(s)x - D\,s \quad (1)$$

$$\frac{dq_n}{dt} = \rho(s) - \mu(q_n)q_n \quad (2)$$

$$\frac{dx}{dt} = \mu(q_n)\,x - D\,x \quad (3)$$

$$\frac{dq_l}{dt} = (\beta q_n - q_l)\mu(q_n) - \gamma\rho(s) \quad (4)$$

$$\frac{dq_f}{dt} = -q_f\,\mu(q_n) + (\alpha+\gamma)\rho(s) \quad (5)$$

The sugar quota q_g can be derived using the following relation [12]

$$q_l + q_f + q_g = 1$$

In equation (1), the concentration of substrate s (nitrate) relates the dilution rate D and influent inorganic nitrogen concentration s_{in} with the absorption rate $\rho(s) = s\rho_m/(s+K_s)$, where ρ_m is the maximum uptake rate and K_s is the half saturation constant for the substrate. The maximum uptake of specific growth rate is given by $\mu(q_n) = \bar{\mu}(1-Q_0/q_n)$, where $\bar{\mu}$ is the theoretical maximum growth rate, Q_0 is the minimum nitrogen quota which allows the growth of microalgae. The parameters α, β and γ represents the coefficient of protein synthesis, fatty acid synthesis and fatty acid mobilization respectively. The initial conditions for Eqns. (1) to (5) are

At $t=0$, $s(t)=s_0$, $q_n(t)=q_{n0}$, $x(t)=x_0$, $q_l(t)=q_{l0}$, $q_f(t)=q_{f0}$ (6)

Using Eq.(1)-(3), the following relation can be derived by multiplying Eq. (2) by $x(t)$, multiplying Eq. (3) by $q_n(t)$, and adding the results to Eq. (1) gives the following linear differential equation

$$\frac{d}{dt}\left(x(t)q_n(t) + s(t) - s_{in}\right) = -D\left(x(t)q_n(t) + s(t) - s_{in}\right) \quad (7)$$

with the exact solution

$$x(t)q_n(t) + s(t) - s_{in} = \left(x(0)q_n(0) + s(0) - s_{in}\right)e^{-Dt} \quad (8)$$

III. NEW APPROACH TO HOMOTOPY PERTURBATION METHOD

The homotopy perturbation was first proposed by He et al [19]. This method is used to find an approximate analytical solution of the linear and nonlinear problems. The homotopy perturbation method is a combination of the perturbation method and homotopy in topology. The benefit of this technique is that it does not need a small parameter in the system, leading to extensive application in nonlinear wave equations [20]. The homotopy perturbation method has been applied to various boundary value problems [21-25]. Recently a new approach to HPM is presented to solve the nonlinear problem and this resulted in a simple approximate solution in the zeroth iteration [26].

IV. ANALYTICAL EXPRESSIONS FOR THE CONCENTRATION OF SUBSTRATE, INTERNAL NITROGEN CELL QUOTA, CONCENTRATION OF BIOMASS, LIPID QUOTA, FUNCTIONAL QUOTA AND SUGAR QUOTA USING NEW APPROACH TO HOMOTOPY PERTURBATION METHOD

In this work, we employed a new approach to Homotopy perturbation (Appendix-A) to solve the non-linear differential equations (1) - (6). Using this method, the analytical expressions of concentration of substrate, $s(t)$ internal nitrogen cell quota, $q_n(t)$, concentration of biomass, $x(t)$, lipid quota, $q_l(t)$, functional quota, $q_f(t)$ and sugar quota, $q_g(t)$ are obtained as follows:

$$s(t) = \frac{D s_{in}}{M} + \left(s_0 - \frac{D s_{in}}{M} \right) e^{-Mt} \tag{9}$$

$$q_n(t) = q_{n0} e^{-\bar{\mu} t} + Q_0 (1 - e^{-\bar{\mu} t}) + \frac{\rho_m x_0}{s_0 + K_s} \left[\frac{D s_{in} (1 - e^{-\bar{\mu} t})}{\bar{\mu} M} + \left(s_0 - \frac{D s_{in}}{M} \right) \frac{e^{-Mt} - e^{-\bar{\mu} t}}{\bar{\mu} - M} \right] \tag{10}$$

$$x(t) = \frac{(x_0 q_0 + s_0 - s_{in}) e^{-Dt} - \left[\frac{D s_{in}}{M} + \left(s_0 - \frac{D s_{in}}{M} \right) e^{-Mt} \right] + s_{in}}{q_{n0} e^{-\bar{\mu} t} + Q_0 (1 - e^{-\bar{\mu} t}) + \frac{\rho_m x_0}{s_0 + K_s} \left[\frac{D s_{in} (1 - e^{-\bar{\mu} t})}{\bar{\mu} M} + \left(s_0 - \frac{D s_{in}}{M} \right) \frac{e^{-Mt} - e^{-\bar{\mu} t}}{\bar{\mu} - M} \right]} \tag{11}$$

$$q_l(t) = q_{l0} e^{-\bar{\mu} t} + \bar{\mu} \beta (q_{n0} - Q_0) t e^{-\bar{\mu} t} + \frac{\rho_m D s_{in}}{M (s_0 + K_s)} \left[\frac{(\beta - \gamma)(1 - e^{-\bar{\mu} t})}{\bar{\mu}} - \beta t e^{-\bar{\mu} t} \right]$$

$$+ \frac{q_{l0} Q_0 (1 - e^{-\bar{\mu} t})}{q_{n0}} - \frac{\rho_m \left(s_0 - \frac{D s_{in}}{M} \right)}{s_0 + K_s} \left[\frac{e^{-Mt} - e^{-\bar{\mu} t}}{(\bar{\mu} - M)^2} - \frac{t e^{-\bar{\mu} t}}{\bar{\mu} - M} - \gamma t e^{-\bar{\mu} t} \right] \tag{12}$$

$$q_f(t) = q_{f0} e^{-\bar{\mu} t} + \frac{q_{f0} Q_0 (1 - e^{-\bar{\mu} t})}{q_{n0}}$$

$$+ \frac{(\alpha + \gamma) \rho_m}{s_0 + K_s} \left[\frac{D s_{in} (1 - e^{-\bar{\mu} t})}{\bar{\mu} M} - \left(s_0 - \frac{D s_{in}}{M} \right) \frac{e^{-Mt} - e^{-\bar{\mu} t}}{\bar{\mu} - M} \right] \tag{13}$$

$$q_g(t) = 1 - \left[q_l(t) + q_f(t) \right] \tag{14}$$

where $M = [\rho_m x_0 + D(s_0 + K_s)] / (s_0 + K_s)$ (15)

Comparison of analytical, experimental and numerical work

In order toprove the usefulness of the present method, the obtained analytical results [equations (9) – (14)] are compared with experimental data [12] and numerical simulation in Figure 2 for all concentrations and quotas for all values of time *t*. Comparison confirmed the steady state value of our analytical results coincides with experimental and numerical results. The numerical solutions are found using pdepe (Finite element method) in Matlab[27]. This Matlab program [28]is given in Appendix B. Graphical results are presented and discussed quantitatively to illustrate the solutions in figures. (2) – (8). An agreement between analytical, experimental and numerical results is noted.

Discussion

Equations (9) - (14) represents the simple approximate analytical expression for the concentrations and quotas. The main variable of interest in this manuscript is the concentration of biomass *x*(*t*). In order to increase the biofuel production, the concentration of biomass of microalgae has to be increased. Further, to analyze the influence of parameters such as growth rate, uptake rate etc., over the concentrations and quotas, the solutions of equations (9) - (14) are plotted in Figure. (3) - (8).

In Figure 3, the concentration of substrate (nitrate) $s(t)$ versus time t for various experimental values of influent nitrogen concentration s_{in}, dilution rate D, maximal uptake rate ρ_m and half saturation constant K_s are plotted. From this figure, it is evident that the concentration of substrate decreases when influent nitrogen concentration and half saturation constantdecreases, whereas the concentration of nitrate increases when dilution rate and the maximal uptake rate decreases. The substrate reaches the steady state value when $t \geq 5$. This steady state value depends upon the influent nitrogen concentration s_{in}.

Figure 4 shows the model prediction for nitrogen quota $q_n(t)$ in lipid production as a function of time t for various values of parameters. Sharp increases are due to large nitrogen input at the beginning. Nitrogen is then consumed due to algae uptake. After 1 day ($t \leq 1$), the nitrogen concentration starts to decrease. From Figures 4(b) - 4(d), it can be confirmed that the nitrogen quota increases when the growth rate and saturation constant decreases. And the variation in uptake rate doesn't so much deviate in nitrogen quota with respect to time [Refer Figure 4(c)].

The change in biomass concentration $x(t)$ versus time t for various values of minimum nitrogen quota Q_0, dilution rate D, maximal uptake rate ρ_m and maximum growth rate $\bar{\mu}$ are shown in Fig. 5. An abrupt increase in biomass concentration in each day is due to the increase in the growth rate of microalgae. After 5 days, the concentration of biomass starts to decrease. This is because, the concentration of nitrogen and uptake of nitrogen by algae decreases. Also decreasing the nitrogen quota and dilution rate increases the biomass concentration.

Fig. 6 indicate the lipid quota $q_l(t)$ versus time t. The lipid quota depends upon the coefficient of fatty acid synthesis β, coefficient of fatty acid mobilization γ, uptake rate $\rho(s)$ and growth rate $\mu(q_n)$. Lipid quota initially shows some fluctuations (decreases and then increases) and reaches the maximum when $t \approx 0.8$. After 1 day, the lipid quota starts to decline due to the

decrease in the concentration of nitrogen. From this figure, it is evident that the lipid quota increases when β increases and γ decreases.

The model results for functional (protein and nucleic acid) quota $q_f(t)$ versus time t for different values of coefficient of protein synthesis α, coefficient of fatty acid mobilization γ, minimum uptake rate ρ_m and maximal growth rate $\bar{\mu}$ are represented in Figure 7. A sudden increase in the quota is due to the increase of the coefficient of protein and fatty acid synthesis. The functional quota increases when the uptake of nitrogen by algae increases. From this figure, it is confirmed that the growth rate of microalgae is inversely proportional to the mass of protein and nucleic acid in the concentration of biomass.

The influence of parameters like coefficient of protein synthesis α, coefficient of fatty acid synthesis β, minimum uptake rate ρ_m and maximal growth rate $\bar{\mu}$ over sugar quota $q_g(t)$ are plotted in Fig. 8. From this figure, it can be concluded that the parameters which control the concentration of sugar in biomass concentration are α and β. Since, increasing the value of α and β decreases the sugar concentration in biomass. Obviously, the growth of microalgae increases the sugar level in the biomass. And for large values of t ($t=10$), the sugar quota reaches its steady state value.

The absorption rate $\rho(s)$ versus concentration of substrate (Nitrate) $s(t)$ and time t are shown in Figure 9. The absorption rate is an increasing function of Nitrate s and decreasing function of time t. Since, the concentration of substrate $s(t)$ reaches its steady state value when $t=5$ [Refer Figure 1(a)], the absorption rate $\rho(s)$ reaches its steady state value at the same time. It reaches its maximum value when $s=0.5$ and $t=0$.

The growth rate $\mu(q_n)$ versus nitrogen quota $q_n(t)$ and time t are shown in Fig. 10. Growth rate is a linearly increasing function of nitrogen quota $q_n(t)$ and reaches the stationary growth phase (growth rate remains constant) when $t=5$. But, it decreases as a function of time t. The growth rate $\mu(q_n)$ reaches its steady state value at $t=5$, where the nitrogen quota reaches its steady state [Refer Fig. 1(b)]. It reaches its maximum value when $q_n=1$ and $t=0$.

Conclusion

A system of time dependent nonlinear differential equations in the microalgal lipid production model has been solved analytically. The main objective of this paper is to provide the analytical expressions for the dynamical model for neutral lipid production by microalgae for biofuel production. Approximate analytical expressions for the concentrations and quotas have been derived using a new approach to HPM. Using this result, the influence of the parameters over growth rate and absorption rate of microalgae can be investigated. The theoretical analysis of our analytical result helps us for the better understanding of the system and to predict the behavior of the system.

Acknowledgements

This work was supported by the Department of Science and Technology, SERB-DST (EMR/2015/002279) Government of India. The Authors are also thankful to Shri J. Ramachandran, Chancellor, Col. Dr. G. Thiruvasagam, Vice-Chancellor, Academy of Maritime Education and Training(AMET), Deemed to be University, for their constant encouragement.

References

[1].Suali, E.; Sarbatly R, 2010. Conversion of microalgae to biofuel. *Renewable and sustainable Energy Reviews*, *16*, 4316-4342.

[2].Lee, J-Y.; Yoo, C.; Jun S-Y.; Ahn, C-Y.; Oh, H.M, 2010. Comparison of several methods for effective lipid extraction from microalgae. *Bioresource Technology*, *10*, 1575-577.

[3].Nigam, P.S.; Singh, A, 2011. Production of liquid biofuels from renewable resources. *Prog. Energ. Combust*. *37*, 52-68.

[4].Benemann, J.R, 2008. Opportunities and Challenges in Algae Biofuels Production. *Algae World* .

[5].Quinn, J.; de Winter, L.; Bradley, T, 2011. Microalgae bulk growth model with application to industrial scale systems. *Bioresource Technology*, *102*, 5083-5092.

[6].Rawat, I.; Kumar, R.; Mutanda, T.; Bux, F, 2013. Biodiesel from microalgae: A critical evaluation from laboratory to large scale production. *Applied Energy*, *103*, 444 - 467.

[7].Bernard, O, 2011. Hurdles and Challenges for modelling and control of microalgae for CO_2 mitigation and biofuel production. *Journal of Process Control*, *21*, 1378-1389.

[8].Ho, S-H.; Huang, S-W.; Chen, C-Y.; Hasunuma, T.; Kondo, A.; Chang, J-S, 2013. Bioethanol production using carbohydrate-rich microalgae biomass as feedstock. *Bioresource Technology*, *135*, 191-198.

[9].Sukenik, A.; Falkowski, P.G.; Bennett, J, 1987. Potential enhancement of photosynthetic energy conversion in algal mass culture. *Biotechnol. Bioeng*, *30*, 970-977.

[10].Sukenik, A.; Levy, R.S.; Levy, Y.; Falkowski, P.G.; Dubinsky, Z, 1991. Optimizing algal biomass production in an outdoor pond: a simulation model. *J. Appl. Phycol*. *3*, 191-201.

[11].Lemesle, V.; Mailleret, L, 2008. A mechanistic investigation of the algae growth "Droop" model. *ActaBiotheor*. *56*, 87-91.

[12].Mairet, F.; Bernard, O.; Masci, P.; Lacour, T.; Sciandra, A, 2011. Modelling neutral lipid production by the microalga *Isochrysis*aff. Galbana under nitrogen limitation. *Bioresource Technology*, *102*, 142-149.

[13].Ross, O.; Geider, R, 2009. New cell-based model of photosynthesis and photo-acclimation: accumulation and mobilization of energy reserves in phytoplankton. *Marine Ecol. Prog. Series*, *383*, 53-71.

[14].Droop, M.R, 1983. 25 years of algal growth kinetics, a personal view. *Botanica Marina*, *16*, 99-112.

[15].Geider, R.; MacIntyre, H.; Kana, T, 1998. A dynamic regulatory model of phytoplanktonic acclimation to light, nutrients and temperature. *LimnolOceanogr*, *43*, 679-694.

[16].Droop, M.R, 1968. Vitamin B12 and marine ecology IV-The kinetics of uptake growth and inhibition in Monochrysislutheri. *J. Mar. Biol. Assoc*. *48*, 689-733.

[17].Sciandra, A.; Ramani, P, 1994. The limitations of continuous cultures with low rates of medium renewal per cell. *J. Exp. Mar. Biol. Ecol*. *178*, 1-15.

[18].Bernard, O.; Gouze, J.L, 1999. Nonlinear qualitative signal processing for biological systems: application to the algal growth in bioreactors. *Math. Biosci*. *157*, 357-372.

[19].He, J-H, 1999. Homotopy perturbation technique. *Compt. Method*. *Appl. Mech. Engg*. *178*, 257-262.

[20].He, J-H, 2005. *Chaos,Solitons and Fractals*, *26*, 695-700.

[21].Hemeda, A.A, 2012. Application of homotopy perturbation method to nonlinear wave equations. *App. Math. Sci.*, *6*, 4787 - 4800.

[22].Ganesan, S.; Anitha, S.; Subbiah, A.; Rajendran, L, 2013. Homotopy perturbation method for solving systems of nonlinear coupled equations. *J. Memb. Biol*. *246*, 435-442.

[23].Meena, A.; Rajendran, L, 2010. Mathematical modeling of amperometric and potetiometric biosensors and system of non-linear equations-Homotopy perturbation approach. *J. Electroanal. Chem*. **2010**, *644*, 50-59.

[24].Eswari, A.; Rajendran, L, 2011. Analytical expressions pertaining to the concentration of catechol-quinone and current at ppo-modified micro-cylinder biosensor for diffusion kinetic model. *J. Electroanal. Chem*. 660, 200-208.

[25]. Venugopal, K.; Eswari, A.; Rajendran, L, 2011. Mathematical model for steady state current at ppo-modified micro-cylinder biosensors. *J. Biomed. Sci. Engg*. 4, 631-641.

[26].Rajendran, L.; Anitha, S, 2013. Reply to "Comments on analytical solution of amperometric enzymatic reactions based on HPM". *Electrochim. Acta*. *102*, 474-476.

[27] Skeel, R.D.; Berzins, M.A, 1990. A method for the spatial discretization of parabolic equations in one space variable. J. Sci. & Stat. Com. 11, 1-32.

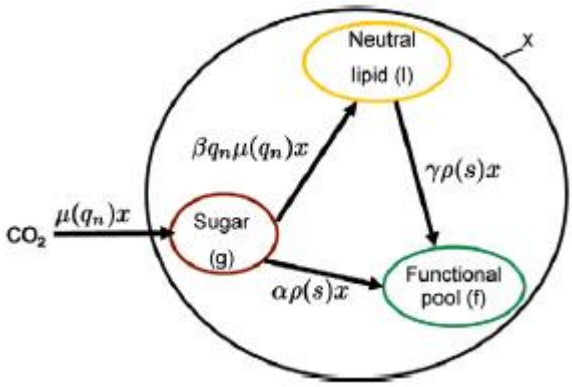

Figure 1. Schematic diagram for carbon flows. The dynamics of neutral lipids results from the unbalance between fatty lipid synthesis and mobilization [12].

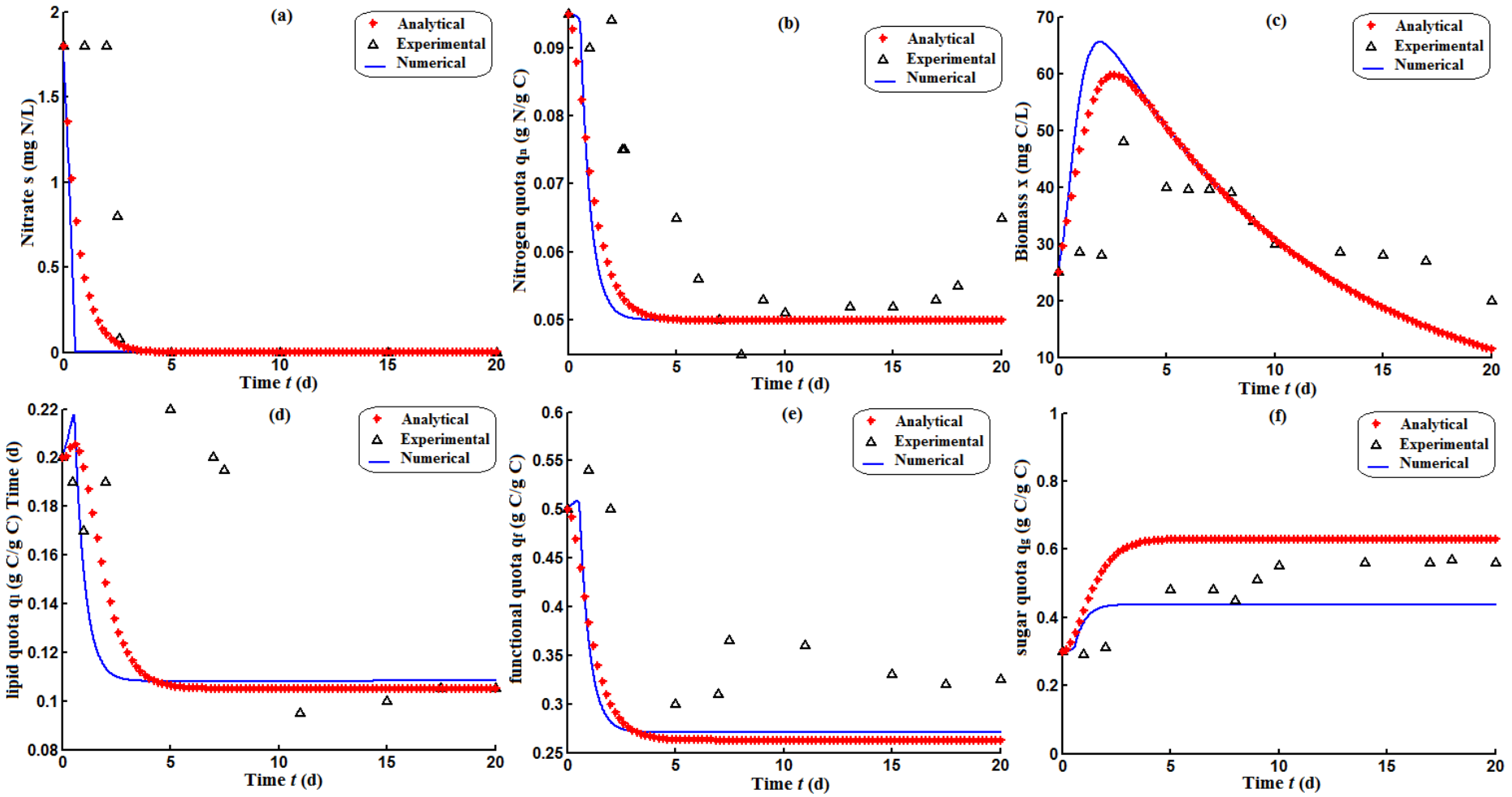

Figure 2. Comparison of analytical results [Eqns. (9)-(14)] for dynamical model of microalgal growth with experimental data [12] and numerical simulation (Matlab program) for fixed values of the experimental parameters (Refer Table. I).

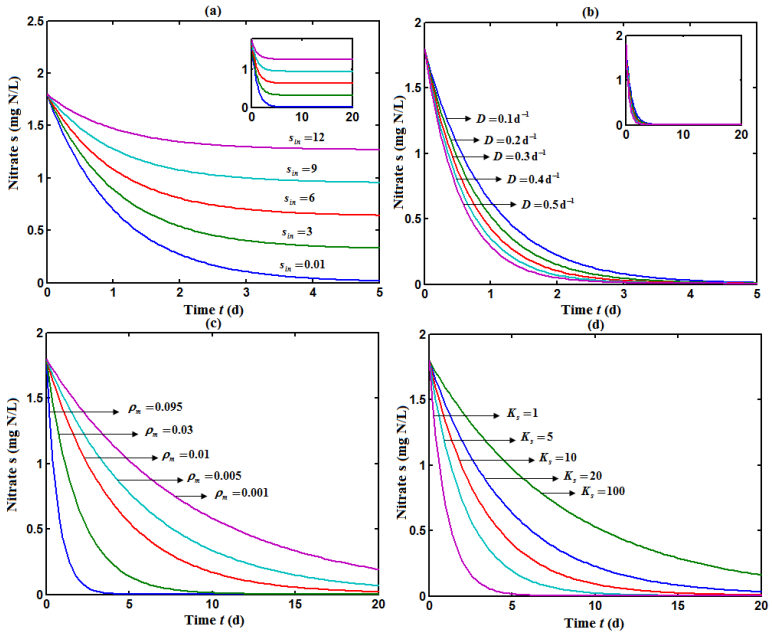

Figure 3. Concentration of nitrogen $s(t)$ versus time t for various values of influent nitrogen concentration s_{in}, dilution rate D, maximal uptake rate ρ_m and half saturation constant K_s and for some fixed values of the parameter (Refer Table. I).

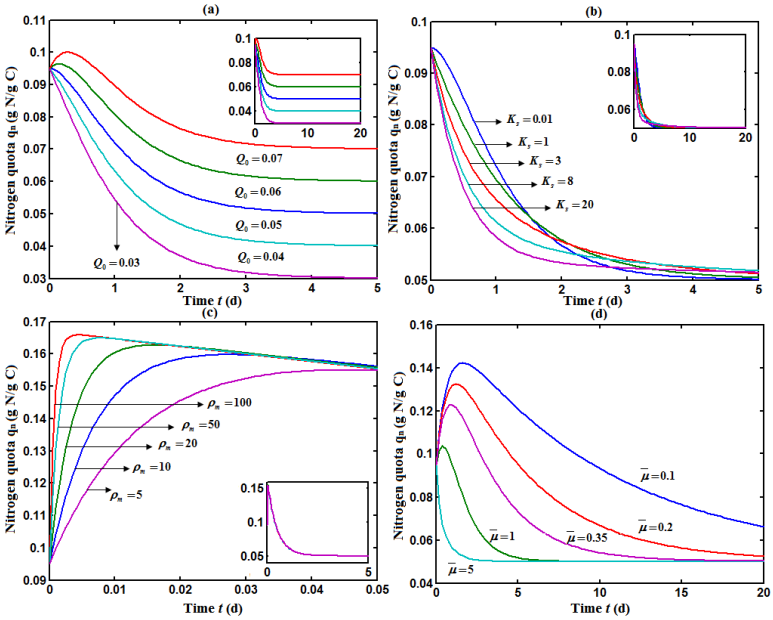

Figure 4. Nitrogen quota $q_n(t)$ versus time t for various values of minimum nitrogen quota Q_0, half saturation constant K_s, maximal uptake rate ρ_m and maximum growth rate $\bar{\mu}$ and for some fixed values of the parameter (Refer Table. I).

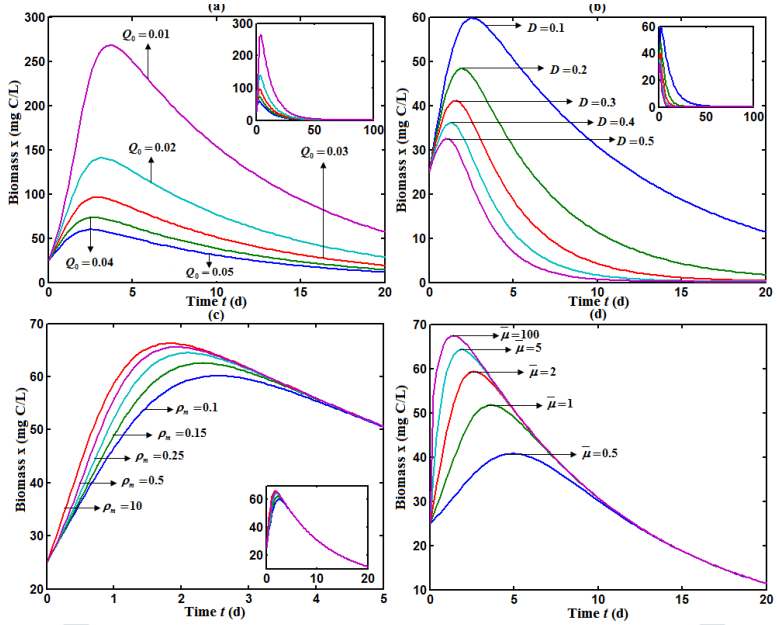

Figure 5. Concentration of biomass $x(t)$ versus time t for various values of minimum nitrogen quota Q_0, dilution rate D, maximal uptake rate ρ_m and maximum growth rate $\bar{\mu}$ and for some fixed values of the parameter (Refer Table. I).

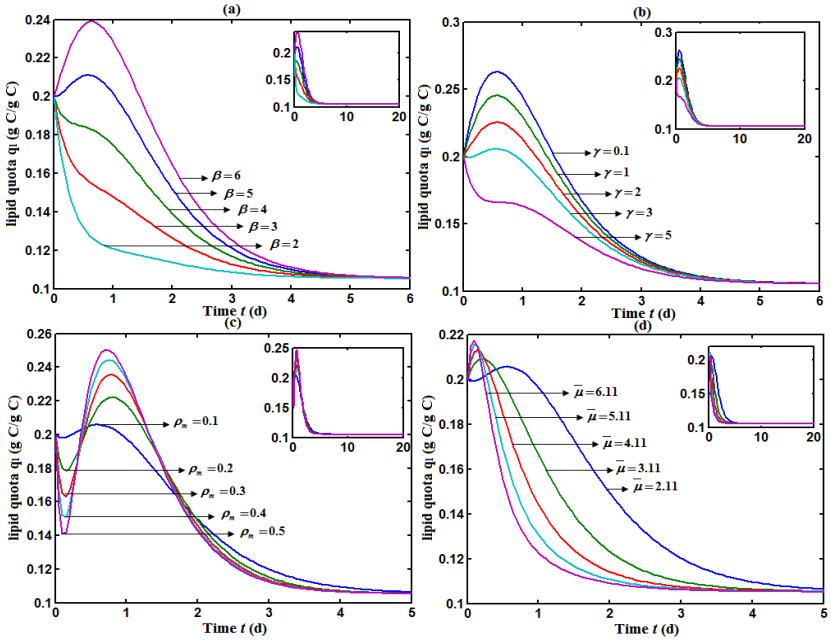

Figure 6. Lipid quota $q_l(t)$ versus time t for various values of fatty acid synthesis coefficient β, fatty acid mobilization coefficient γ, maximal uptake rate ρ_m and maximum growth rate $\bar{\mu}$ and for some fixed values of the parameter (Refer Table. I).

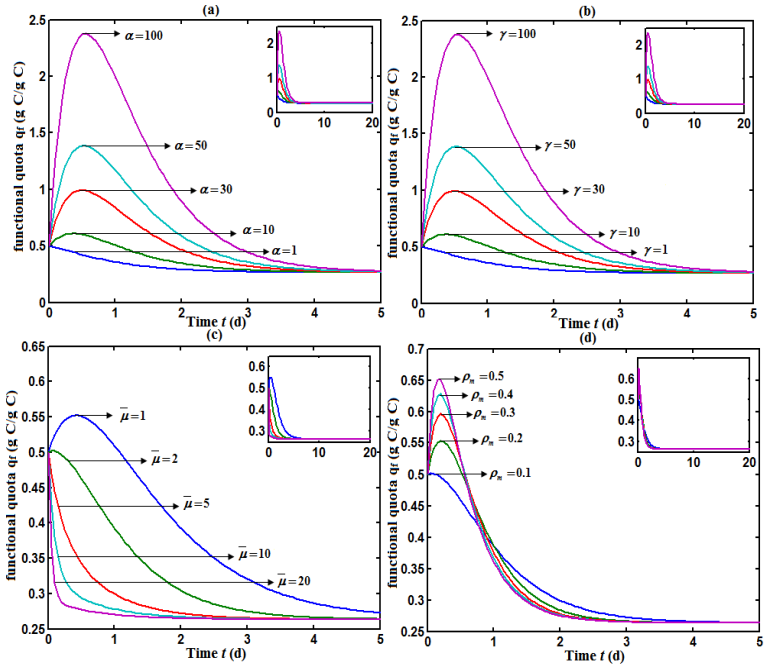

Figure 7. Functional quota $q_f(t)$ versus time t for various values of protein synthesis coefficient α, fatty acid mobilization coefficient γ, maximal uptake rate ρ_m and maximum growth rate $\bar{\mu}$ and for some fixed values of the parameter (Refer Table. I).

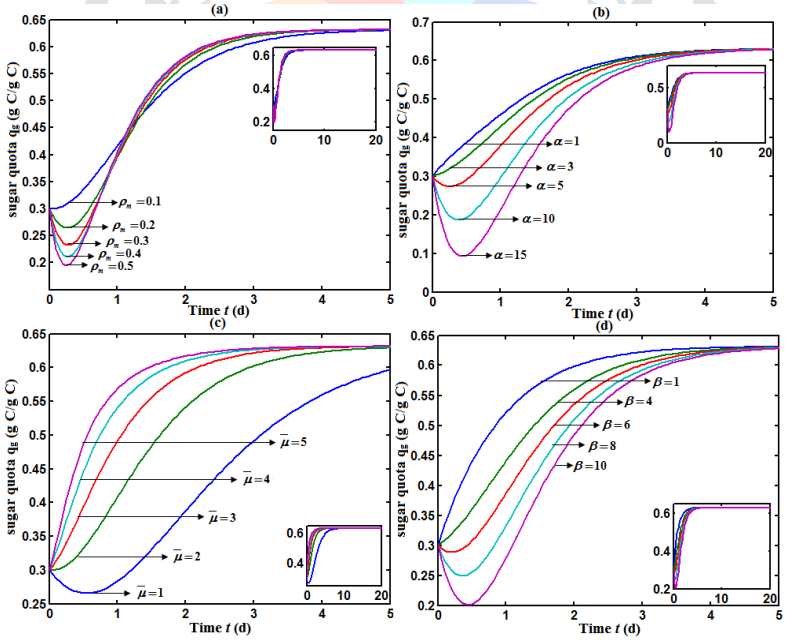

Figure 8. Sugar quota $q_n(t)$ versus time t for various values of maximal uptake rate ρ_m, protein synthesis coefficient α, maximum growth rate $\bar{\mu}$ and fatty acid synthesis coefficient β and for some fixed values of the parameter (Refer Table. I).

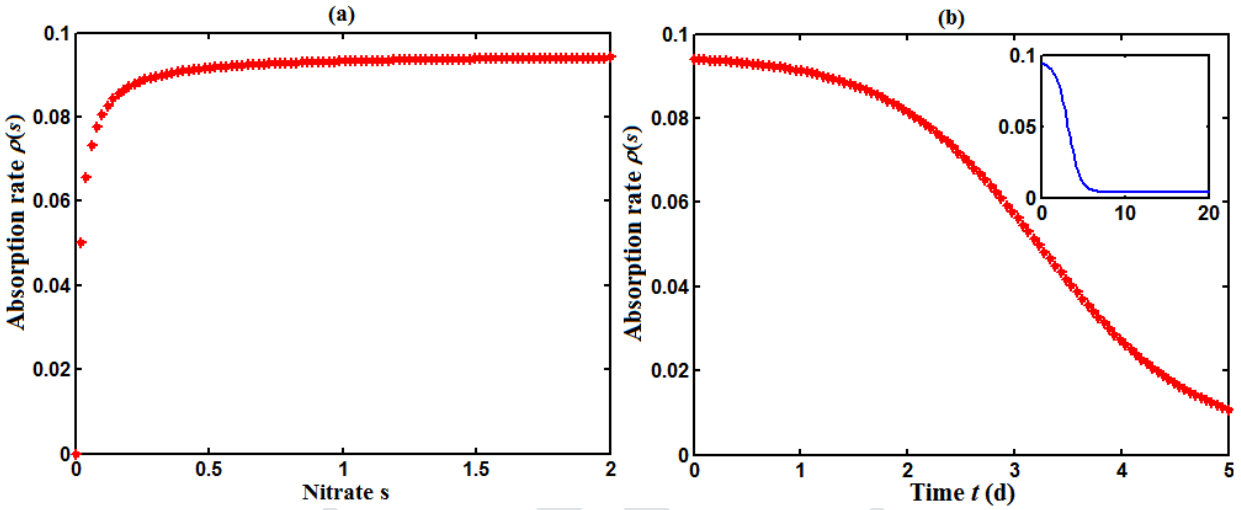

Figure 9. Profile of absorption rate $\rho(s)$ versus time for some fixed values of the parameter (Refer Table. I).

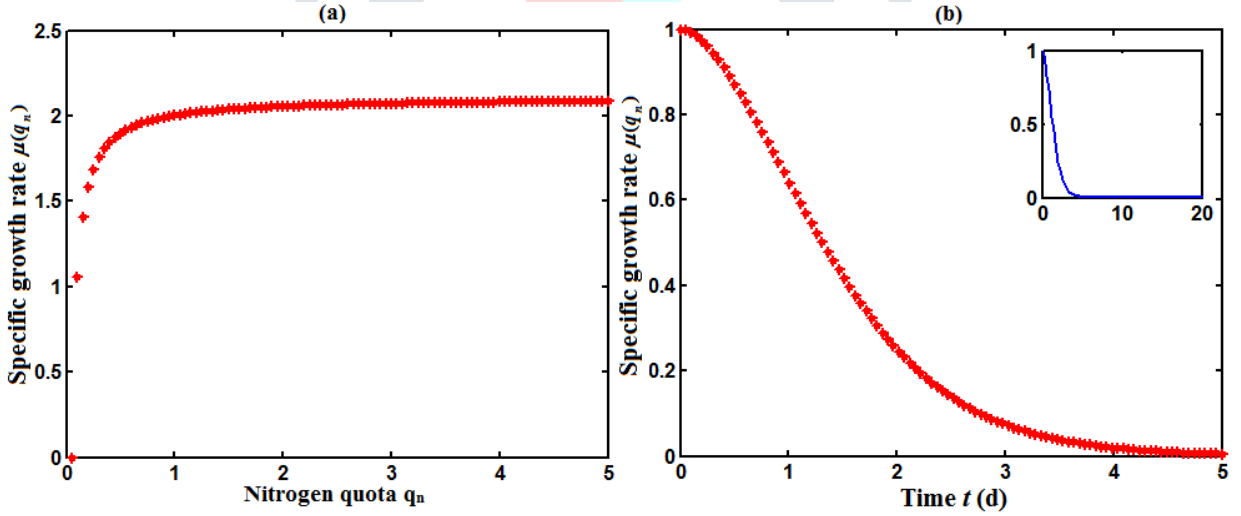

Figure 10. Profile of specific growth rate $\mu(q_n)$ versus time for some fixed values of the parameter (Refer Table. I).

Appendix A

Approximate analytical solution of the nonlinear Eqns. (1) – (5) using new approach to Homotopy perturbation method

In this appendix, we have indicated how to find the solution of Eqns. (1) – (5) using the initial condition Eqn. (6). In order to solve Eqns. (1) - (5), we first construct the homotopy for the equations as follows:

$$(1-p)\left\{\frac{ds}{dt}+D(s-s_{in})+\frac{\rho_m x(0)s}{s(0)+K_s}\right\}+p\left\{(s+K_s)\left[\frac{ds}{dt}+D(s-s_{in})\right]+\rho_m sx\right\}=0 \quad (A.1)$$

$$(1-p)\left\{\frac{dq_n}{dt}+\overline{\mu}\left(1-\frac{Q_0}{q_n}\right)q_n-\frac{\rho_m s_{zeroth}}{s(0)+K_s}\right\}+p\left\{(s+K_s)\left[\frac{dq_n}{dt}+\overline{\mu}(q_n-Q_0)\right]-\rho_m s\right\}=0 \quad (A.2)$$

$$(1-p)\left\{\frac{dx}{dt}+Dx-\overline{\mu}\left(1-\frac{Q_0}{q_n(0)}\right)x\right\}+p\left\{q_n\left(\frac{dx}{dt}+Dx\right)-\overline{\mu}(q_n-Q_0)x\right\}=0 \quad (A.3)$$

$$(1-p)\left\{\frac{dq_l}{dt}+\overline{\mu}q_l-\overline{\mu}\beta(q_{nzeroth}-Q_0)+\frac{\gamma\rho_m s_{zeroth}}{s(0)+K_s}-\frac{\overline{\mu}Q_0q_l(0)}{q_n(0)}\right\}$$
$$+p\left\{(s+K_s)\left[\frac{dq_l}{dt}+\overline{\mu}q_l-\overline{\mu}\beta(q_n-Q_0)-\frac{\overline{\mu}Q_0q_l}{q_n}+\gamma\rho_m s\right]\right\}=0 \quad (A.4)$$

$$(1-p)\left\{\frac{dq_f}{dt}+\overline{\mu}q_f-\frac{\overline{\mu}Q_0q_f(0)}{q_n(0)}-\frac{(\alpha+\gamma)\rho_m s_{zeroth}}{s(0)+K_s}\right\}$$
$$+p\left\{(s+K_s)\left(\frac{dq_f}{dt}+\overline{\mu}q_f-\frac{\overline{\mu}Q_0q_f}{q_n}\right)-(\alpha+\gamma)\rho_m s\right\}=0 \quad (A.5)$$

The approximate solution of Eqns. (A.1) to (A.5) is

$$\begin{cases} s=s_{zeroth}+ps_{first}+p^2s_{second}+\ldots \\ q_n=q_{n\,zeroth}+pq_{n\,first}+p^2q_{n\,second}+\ldots \\ x=x_{zeroth}+px_{first}+p^2x_{second}+\ldots \\ q_l=q_{l\,zeroth}+pq_{l\,first}+p^2q_{l\,second}+\ldots \\ q_f=q_{f\,zeroth}+pq_{f\,first}+p^2q_{f\,second}+\ldots \end{cases} \quad (A.6)$$

Substituting equation (A6) into equations. (A.1) – (A.4) and arranging the coefficients of powers p

$$p^0:\frac{ds_{zeroth}}{dt}+D(s_{zeroth}-s_{in})+\frac{\rho_m x(0)s_{zeroth}}{s(0)+K_s}=0 \quad (A.7)$$

$$p^0:\frac{dq_{n\,zeroth}}{dt}+\overline{\mu}\left(q_{n\,zeroth}-Q_0\right)-\frac{\rho_m s_{zeroth}}{s(0)+K_s}=0 \quad (A.8)$$

$$p^0:\frac{dx_{zeroth}}{dt}+Dx_{zeroth}-\overline{\mu}\left(1-\frac{Q_0}{q_n(0)}\right)x_{zeroth}=0 \quad (A.9)$$

$$p^0:\frac{dq_{l\,zeroth}}{dt}+\overline{\mu}q_{l\,zeroth}-\overline{\mu}\beta(q_{nzeroth}-Q_0)+\frac{\gamma\rho_m s_{zeroth}}{s(0)+K_s}-\frac{\overline{\mu}Q_0q_l(0)}{q_n(0)}=0 \quad (A.10)$$

$$p^0:\frac{dq_{f\,zeroth}}{dt}+\overline{\mu}q_{f\,zeroth}-\frac{\overline{\mu}Q_0q_f(0)}{q_n(0)}-\frac{(\alpha+\gamma)\rho_m s_{zeroth}}{s(0)+K_s}=0 \quad (A.11)$$

The initial conditions in Eqn. (6) becomes

At $t=0$,

$$s_{zeroth}(0)=s_0,\ q_{n\,zeroth}(0)=q_{n0},\ x_{zeroth}(0)=x_0,\ q_{l\,zeroth}(0)=q_{l0},\ q_{f\,zeroth}(0)=q_{f0} \quad (A.12)$$

and

$$s_i(0)=s_0, q_{ni}(0)=q_{n0}, x_i(0)=x_0, q_{li}(0)=q_{l0}, q_{fi}(0)=q_{f0}, \forall i=first, second, third\ldots \quad (A.13)$$

Solving the Eqns. (A.7) – (A.11) for the initial condition (A.12), we can find the following results

$$s_{zeroth}(t)=\frac{D\,s_{in}}{M}+\left(s_0-\frac{D\,s_{in}}{M}\right)e^{-Mt} \quad (A.14)$$

$$q_{n\,zeroth}(t)=q_{n0}e^{-\overline{\mu}t}+Q_0(1-e^{-\overline{\mu}t})+\frac{\rho_m\,x_0}{s_0+K_s}\left[\frac{D\,s_{in}(1-e^{-\overline{\mu}t})}{\overline{\mu}M}+\left(s_0-\frac{D\,s_{in}}{M}\right)\frac{e^{-Mt}-e^{-\overline{\mu}t}}{\overline{\mu}-M}\right] \quad (A.15)$$

Substituting euqation (A.14) and (A.15) in the relation, we get $x_{zeroth}(t)$ as follows:

$$x_{zeroth}(t) = \frac{(x_0 q_0 + s_0 - s_{in})e^{-Dt} - \left[\frac{D s_{in}}{M} + \left(s_0 - \frac{D s_{in}}{M}\right)e^{-Mt}\right] + s_{in}}{q_{n0}e^{-\bar{\mu}t} + Q_0(1-e^{-\bar{\mu}t}) + \frac{\rho_m x_0}{s_0 + K_s}\left[\frac{D s_{in}(1-e^{-\bar{\mu}t})}{\bar{\mu} M} + \left(s_0 - \frac{D s_{in}}{M}\right)\frac{e^{-Mt} - e^{-\bar{\mu}t}}{\bar{\mu} - M}\right]} \quad \text{(A.16)}$$

$$q_{l\,zeroth}(t) = q_{l0}e^{-\bar{\mu}t} + \bar{\mu}\beta(q_{n0} - Q_0)te^{-\bar{\mu}t} + \frac{\rho_m D s_{in}}{M(s_0 + K_s)}\left[\frac{(\beta-\gamma)(1-e^{-\bar{\mu}t})}{\bar{\mu}} - \beta te^{-\bar{\mu}t}\right]$$
$$+ \frac{q_{l0}Q_0(1-e^{-\bar{\mu}t})}{q_{n0}} - \frac{\rho_m\left(s_0 - \frac{D s_{in}}{M}\right)}{s_0 + K_s}\left[\frac{e^{-Mt} - e^{-\bar{\mu}t}}{(\bar{\mu} - M)^2} - \frac{te^{-\bar{\mu}t}}{\bar{\mu} - M} - \gamma te^{-\bar{\mu}t}\right] \quad \text{(A.17)}$$

$$q_{f\,zeroth}(t) = q_{f0}e^{-\bar{\mu}t} + \frac{q_{f0}Q_0(1-e^{-\bar{\mu}t})}{q_{n0}}$$
$$+ \frac{(\alpha+\gamma)\rho_m}{s_0 + K_s}\left[\frac{D s_{in}(1-e^{-\bar{\mu}t})}{\bar{\mu} M} - \left(s_0 - \frac{D s_{in}}{M}\right)\frac{e^{-Mt} - e^{-\bar{\mu}t}}{\bar{\mu} - M}\right] \quad \text{(A.18)}$$

Where M is given in the equation (19). Similarly, we can find the next iteration to improve the accuracy of the solution.

Appendix B

Matlab program to find the numerical solution of Eqns. (1) - (6)

```
function graphmain3
options= odeset('RelTol',1e-6,'Stats','on');
%initial conditions
Xo = [1.8; 0.095; 25; 0.2; 0.5; 0.3];
tspan = [0 20];
tic
[t,X] =ode45(@TestFunction,tspan,Xo,options);
toc
figure
hold on
%plot(t, X(:,1),'-')
%plot(t, X(:,2),'-')
%plot(t, X(:,3),'-')
%plot(t, X(:,4),'-')
%plot(t, X(:,5),'-')
plot(t, X(:,6),'-')legend('x1','x2','x3','x4','x5','x6')
ylabel('x')
xlabel('t')
```

```
return

function [dx_dt]= TestFunction(t, x)

D=0.1;sn=0.01;ks=0.018;pm=0.095;Qo=0.05;mu=2.11;b=4.8;v=3;a=2.6;

dx_dt(1) =D*sn-(pm*x(1)*x(3))/(x(1)+ks)-D*x(1);

dx_dt(2) =(pm*x(1))/(x(1)+ks)-mu*(1-Qo/x(2))*x(2);

dx_dt(3) =mu*(1-Qo/x(2))*x(3)-D*x(3);

dx_dt(4) =-((b*x(2)-x(4))*mu*(1-Qo/x(2))-v*(pm*x(1))/(x(1)+ks));

dx_dt(5) =-x(5)*mu*(1-Qo/x(2))+(a+v)*(pm*x(1))/(x(1)+ks);

dx_dt(6) =(-(((b*x(2)-x(4))*mu*(1-Qo/x(2))-v*(pm*x(1))/(x(1)+ks))+(-x(5)*mu*(1-Qo/x(2))+(a+v)*(pm*x(1))/(x(1)+ks))));

dx_dt = dx_dt';

return
```

Table I. Nomenclature and values of the parameter used in the model

Parameter	Description	Values	Units
CO_2	Carbon dioxide	—	g
D	Dilution rate	0.1	d^{-1}
K_s	Half saturation constant for substrate	0.08	d^{-1}
Q_0	Minimum nitrogen quota	0.05	mg[N] mg[C] -1
q_f	Functional Quota	—	g C/g C
q_{f0}	Initial value of functional Quota	0.5	g C/g C
q_g	Sugar quota	—	g C/g C
q_{g0}	Initial value of sugar quota	—	g C/g C
q_l	Lipid quota	—	g C/g C
q_{l0}	Initial value of lipid quota	—	g C/g C
q_n	Internal nitrogen quota	—	g N/g C
q_{n0}	Initial value of internal nitrogen quota	0.095	g N/g C
s	Concentration of nitrate	—	mg N/L
s_0	Initial concentration of nitrate	1.8	mg/L
s_{in}	Influent inorganic nitrogen concentration	0.01	mg/L
x	Concentration of biomass	—	mg C/L
x_0	Initial concentration of biomass	25	mg C/L
Greek Symbols			
α	Coefficient of protein synthesis	2.6	mg[C] mg[N]-1
β	Coefficient of fatty acid synthesis	4.8	mg[C] mg[N]-1
γ	Coefficient of fatty acid mobilizati on	3	mg[C] mg[N]-1
$\bar{\mu}$	Theoretical maximum growth rate	2.11	d -1
ρ_m	Maximum uptake rate	0.095	mg[N] mg[C]-1 d -1
Subscripts	**Grouping parameters**		

n	Cellular nitrogen	$M = [\rho_m x_0 + D(s_0 + K_s)]/(s_0 + K_s)$
l	Neutral lipid reserve compartment	
f	Functional compartment	
g	Sugar reserve compartment	
in	Influent nitrogen	
m	Maximum	
0	Minimum	
s	Substrate	